Study on Denoise Algorithm for Micro-motion Target

Saiqiang Xia[1,a], Wenfei Chen[1], Chaowei Zhang[1], Xiaonan Wang[1] and Dahan Xu[2]

[1.] Air Force Early Warning Academy,Wuhan,430019,China
[2.] Unit 95438 of the PLA,Pengshan,620860,China

[a] xiasaiqiang163.com

Abstract. Aiming at the non-stationary characteristics of narrowband radar echo of micro-motion target, a novel micro-motion signal denoising algorithm is proposed. Firstly, the weight function is constructed by coherent accumulation, and the echo is weighted by weight function to filter out the noise in range dimension. Secondly, the singular spectrum analysis(SSA) is performed on the range bin of the echo, the signal with large singularities is preserved, and the noise with small singularities is filtered out. Then, the azimuth dimension signal transformed from time domain into time-frequency domain, the step iteration method is used to adaptively filter the time-frequency spectrum and the time-frequency filtering result with the best denoising effect selected by defining the risk function. Finally, the simulation verify the effect of the proposed method.

1. Introduction

Radar echo is usually affected by range, RCS or interference environment, the low SNR greatly interfere with the detection of effective signal and the extraction of related features. Therefore, it is necessary to separate the effective signal from the noise. Because of the non-stationarity of the micro-motion signal, the traditional denoising method has a poor effect on the suppression of the noise. For example, the denoise method based on Hilbert-Huang transform (HHT) proposed in [1] is mainly effective for periodic stationary signals, but not for non-stationary signals with spikes or mutations. The denoise method based on Wavelet (WT) proposed in [2-3], which can effectively distinguish noise, but this method needs to select a suitable wavelet basis, and can't eliminate the defects caused by fourier transform. Empirical mode decomposition (EMD) mentioned in [4-7] can deal with non-stationary signals well, but it has some shortcomings such as mode aliasing, endpoint effect, and there will be a lot of noise residues. The method based on ensemble empirical mode decomposition (EEMD) proposed in [8-9] can solve the shortcomings of EMD, but it can't completely remove the noise with the same frequency component as the signal. In [10-11], a threshold denoising method based on time-frequency coefficients is studied, the essence of this method is time-frequency filtering, but its denoising effect is poor in low SNR. Therefore, the denoise method of the rotor target echo still needs to be further studied.

In order to solve the above problems, a novel denoise algorithm is proposed. Firstly, the weighting function is constructed by coherent accumulation, and the range dimension is weighted to achieve the range dimension denoising. Then, the echo with larger singular value is extracted and the noise with smaller singular value is removed by the SSA in the azimuth dimension. Then STFT analysis transform the time domain into time-frequency domain. Time-frequency filtering is carried out by step iteration method, and the risk function is defined. When the risk function takes the local minimum at the first time, the time-frequency result is the final denoise result. Compared with other traditional algorithms, this algorithm has better denoise effect, and finally obtains its time-frequency results, which can provide conditions for subsequent feature extraction.

2. Denoise algorithm in range dimension

The echo of the rotor target after pulse compression can be expressed [12,13] as

$$S(\hat{t},t_m)=\sum_{i=0}^{G}\sum_{j=0}^{N}\sigma_{ij}\mathrm{A}T_{\mathrm{p}}\exp[-j\frac{4\pi}{\lambda}R_{ij}(t_m)]\sin c[B(\hat{t}-\frac{2R_{ij}(t_m)}{c})] \tag{1}$$

In (1), G donates the number of blades; i is expressed as the i th blade on the rotor; N is the number of scattering points on the target single blade; j is expressed as the j th scattering point on the blade; σ_{ij} is the scattering coefficient at the scattering point; B is signal bandwidth; λ is signal wavelength; $R_{ij}(t_m)$ is the range from scattering point to radar.

Under the background of noise, radar echo after pulse compression can be expressed as

$$S_r(\hat{t},t_m)=S(\hat{t},t_m)+N(\hat{t},t_m) \tag{2}$$

Based on narrow-band radar, in the case of short observation time, the rotor target is in the same range bin, but in the case of low SNR, the range bin of the rotor target can't be detected directly. Based on the fact that the echo of the rotor target can be accumulated coherently and the noise can't be accumulated, the fourier transform of the echo is carried out, and the maximum amplitude of the echo after the coherent accumulation is taken out. Then all the amplitudes are normalized, and the weight function is constructed. The echo is weighted to achieve the effect of range dimension noise reduction. Firstly, the weight function is constructed as

$$h(\hat{t})=\frac{\max\left|fft[S_r(\hat{t},t_m)]\right|}{\max\limits_{\hat{t}}\left\{\max\left|fft[S_r(\hat{t},t_m)]\right|\right\}} \tag{3}$$

Weighted processing of echo, it can be writen as

$$S_r'(\hat{t},t_m)=h(\hat{t})\cdot S_r(\hat{t},t_m) \tag{4}$$

The weight function is constructed as shown in Figure 1.

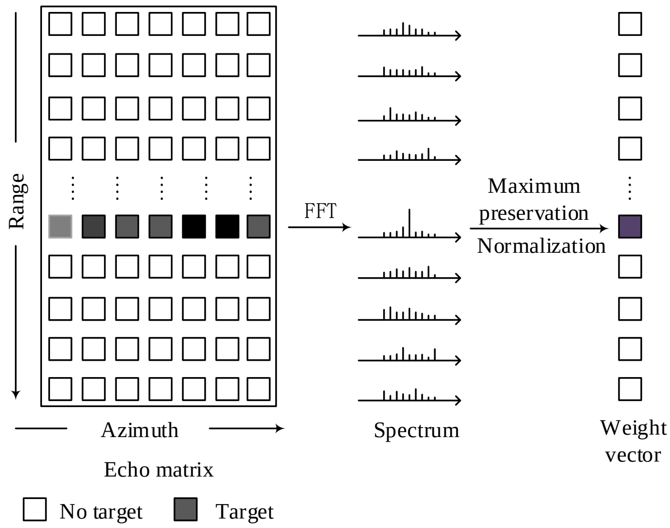

Figure 1. Schematic diagram of weight function construction

Using this method can obtain a large SNR gain, which is related to the number of pulses. Rotor targets can be detected in strong noise background by denoising in range dimension. But the SNR don't change in the range bin which target exist, therefore, it is necessary to reduce noise in this range bin.

3. Denoise algorithm in azimuth dimension

The azimuth dimension denoising algorithm proposed in this paper consists of two steps. The first step is to take out the rang bin of the rotor target on the basis of the range dimension denoising, and process it with SSA in the time domain. The second step is transformed the signal into time-frequency domain, and then adaptive time-frequency filtering is performed to reduce the noise furtherly. Mean square error of the time-frequency matrix of the signal after azimuth dimension denoising and the time-frequency matrix of the signal without adding noise is defined to judge the denoising performance of this algorithm.

3.1. SSA denoise algorithm in time domain

SSA is a linear correlation method based on covariance matrix [14], which can process non-stationary signals. The algorithm distinguishes signals of different components in the original time series by extracting the principal components of signal. The signal is processed by SSA, firstly, the trajectory matrix is constructed according to the observed time series, and the azimuth dimension signal is extracted $\boldsymbol{X}=[x_1,x_2,\ldots,x_M]$, the reconstructed vector $\boldsymbol{X_i}=[x_{(i-1)\tau+1},x_{(i-1)\tau+2},\ldots,x_{L+(i-1)\tau+1}],i=1,2,\ldots,m$ is embedded in dimension m according to a certain delay τ, where $L=M-(i-1)\tau-1$. The m vector is constructed into a $L\times m$ dimensional trajectory matrix $\boldsymbol{T}$.

$$\boldsymbol{T}=\begin{bmatrix}\boldsymbol{X}_1\\ \boldsymbol{X}_2\\ \vdots\\ \boldsymbol{X}_m\end{bmatrix}=\begin{bmatrix}x_1 & x_2 & \cdots & x_{L+1}\\ x_{\tau+1} & x_{\tau+2} & \cdots & x_{L+\tau+1}\\ \vdots & \vdots & & \vdots\\ x_{(m-1)\tau+1} & x_{(m-1)\tau+2} & \cdots & x_M\end{bmatrix} \tag{5}$$

Then the trajectory matrix is decomposed by singular value decomposition (SVD). When constructing the trajectory matrix, it usually satisfies $m<L$. Therefore, the trajectory matrix can be expressed as

$$\boldsymbol{T}=\boldsymbol{U\lambda V^H} \tag{6}$$

In the formula, $\boldsymbol{\lambda}$ is a singular value matrix of $L\times m$ dimension, its principal diagonal element is λ_i, and other elements are zero, that is $\boldsymbol{\lambda}=diag[\lambda_1,\lambda_2,\ldots,\lambda_m]$, $\lambda_1\ge\lambda_2\ge\ldots\ge\lambda_m\ge0$, $\boldsymbol{U}$ is row eigenvector of $\boldsymbol{\lambda}$, and $\boldsymbol{V^H}$ is the column eigenvector of $\boldsymbol{\lambda}$. Take the singular spectrum as

$$\xi_i=\frac{\lambda_i}{\frac{1}{m}\sum_{k=1}^{m}\lambda_k} \tag{7}$$

Singular value represents the relative relationship between the energy of signal and noise in the singular spectrum. The larger ξ_i represents the greater variance of $\boldsymbol{X}$ in feature space, the more information it contains. Generally, larger singular values represent useful information, while smaller singular values represent noise in signals. Partial noise removal by selecting larger singular values.

$$\xi_i=\begin{cases}\xi_i,\xi_i>\frac{1}{m}\sum_{k=1}^{m}\xi_k\\ 0\qquad\quad ,else\end{cases} \tag{8}$$

A new singular value matrix $\boldsymbol{\Sigma}=diag[\xi_1,\xi_2,\ldots,\xi_m]$ is used to reconstruct the trajectory matrix after denoising.

$$\boldsymbol{T'}=\boldsymbol{U\Sigma V^H} \tag{9}$$

Then the azimuth dimension signal $\boldsymbol{X'}$ after denoise is recovered by $\boldsymbol{T'}$. The SSA algorithm can effectively remove the noise. But the effect of noise suppression is poor in frequency band where signal and noise are mixed together, so it is necessary to suppress the noise furtherly.

3.2. Adaptive threshold time-frequency filtering denoise algorithm in time-frequency domain

Generally, the time-frequency analysis is used to obtain the corresponding characteristics of the rotor target, therefore, the echo can be denoised in time-frequency domain. In this paper, an adaptive threshold time-frequency filtering method based on STFT is proposed in order to solve the problem of noise residue after SSA.

Firstly, discrete STFT transform is applied to $\boldsymbol{X}'$ to obtain its time-frequency spectrum.

$$\boldsymbol{STFT}(r,n)=\sum_{k=-\infty}^{+\infty}x'(k)\gamma^*(kT-rT)\exp(-j2\pi(nF)k) \tag{10}$$

$\gamma(\cdot)$ denotes window function, and "*" denotes complex conjugation. $T>0, F>0$ is the sampling period of time and frequency variables, r,n are integers.

$\boldsymbol{STFT}(r,n)$ is a complex matrix, if the real part or imaginary part of the signal is filtered separately, the phase of the signal will be affected. Therefore, this paper considers filtering based on the modulus of time-frequency spectrum coefficients. When adaptive time-frequency filtering is performed, the optimal filtering threshold δ'_{th} must be in the range of $[0,\max(|\boldsymbol{STFT}(r,n)|)]$. How to find the optimal threshold δ'_{th} is the key of this algorithm, if the threshold δ_{th} is small, the noise will not be removed effectively, if δ_{th} is large, the signal will be lost. In view of this situation, this paper uses step iteration method to find δ'_{th}.

Simply set the modulus interval of the spectrum coefficient to $[\alpha,\beta]\max(|\boldsymbol{STFT}(r,n)|), 0\le\alpha<\beta\le 1$, divide $[\alpha,\beta]$ into K steps, the step size of each coefficient is $\Delta d=(\beta-\alpha)/K$, then the step size of the corresponding threshold is

$$\Delta D=\Delta d\max(|\boldsymbol{STFT}(r,n)|) \tag{11}$$

Initialize the threshold as $\delta_{th}=\alpha\max(|\boldsymbol{STFT}(r,n)|)$, the threshold δ_{th} increases with step ΔD to get a new threshold δ_{th-new}. The new threshold is used to filter the time-frequency spectrum and obtain a new spectrum.

$$\boldsymbol{STFT}'(r,n)=\begin{cases}\boldsymbol{STFT}(r,n), & \delta_{th-new}\le|\boldsymbol{STFT}(r,n)|\\ 0 & ,else\end{cases} \tag{12}$$

The purpose of adaptive threshold time-frequency filtering of time-frequency spectrum is to minimize the mean square error of the denoised spectrum with the clean spectrum. However, noise-free signal can't be obtained in the actual processing, its unable to calculate the mean square error of $\boldsymbol{STFT}'(r,n)$ and $\boldsymbol{STFT}_{con}(r,n)$. Therefore, in this paper, the risk function L2-RISK is minimized by calculating the mean square error between the time-frequency spectrum after different threshold processing, and the risk function is defined as

$$R(s)=E\left\|\boldsymbol{STFT}_s(r,n)-\boldsymbol{STFT}_{s-1}(r,n)\right\|_2^2=\frac{1}{r}\frac{1}{n}\sum_{i=1}^{r}\sum_{j=1}^{n}\left|\boldsymbol{STFT}_s(i,j)-\boldsymbol{STFT}_{s-1}(i,j)\right|^2 \tag{13}$$

K values of risk function can be obtained by changing the threshold according to step ΔD. When the first local minimum value of K is obtained, the corresponding threshold is the best threshold, and the best denoising effect can be achieved. Obviously, the optimal threshold δ'_{th} is related to the selection of step size and threshold interval. Generally, the interval can be set as $[\alpha,\beta]=[0.1,0.6]$ [11].

The processing flow of denoise algorithm in azimuth dimension is as follows:

Step 1: Obtain the azimuth dimension array $\boldsymbol{X}$, determine the embedding dimension [15-16], and construct the trajectory matrix $\boldsymbol{T}$.

Step 2: Reduce the rank of $\boldsymbol{T}$ by SVD, and reconstruct the azimuth array $\boldsymbol{X}'$.

Step 3: The time-frequency spectrum $\boldsymbol{STFT}(r,n)$ is obtained by STFT of the $\boldsymbol{X}'$.

Step 4: The iteration range of adaptive threshold δ_{th} is set as $[0.1,0.6]\max(|\boldsymbol{STFT}(r,n)|)$, iteration step is ΔD. The time-frequency spectrum is filtered adaptively by step iteration method, and the new spectrum $\boldsymbol{STFT}'(r,n)$ is obtained.

Journal of Physics: Conference Series **1438** (2020) 012023 doi:10.1088/1742-6596/1438/1/012023

Step 5: Define risk function $R(s)$, calculate mean square errors of spectrum obtained by different threshold processing, the threshold corresponding to the first local minimum is chosen as the optimal threshold δ'_{th}. At this time, the new spectrum is the result of azimuth dimension denoising.

4. Simulation analysis

The simulation chooses 10 scattering points of three rotor blades. The model is shown in Figure 2. The blade length $l = 6\text{m}$, and the SNR defined in this paper is the SNR after pulse compression. Specific simulation parameters are shown in Table 1.

Table 1. Simulation parameters

PRF	τ	B	f_s	T_a
4000Hz	100μs	1MHz	2 MHz	0.512s

Figure 3 is the echo after pulse compression at SNR=3dB. Figure 4 is the result of range dimension weighting of Figure 3. Figure 5 is the STFT result of the range bin which contains the target in Figure 4. Figure 6 is SSA denoise result.Figure 7 is a risk function curve of adaptive threshold filtering for the time-frequency results after SSA denoise, and the number of iterations is 200. Figure 8 is the best denoising result after adaptive threshold time-frequency filtering. Figure 9 is the RMS error of the time-frequency results after denoise method mentioned in this paper , wavelet denoising [2] (method 1), frequency domain denoise [17] (method 2) and EEMD denoise [8] (method 3).

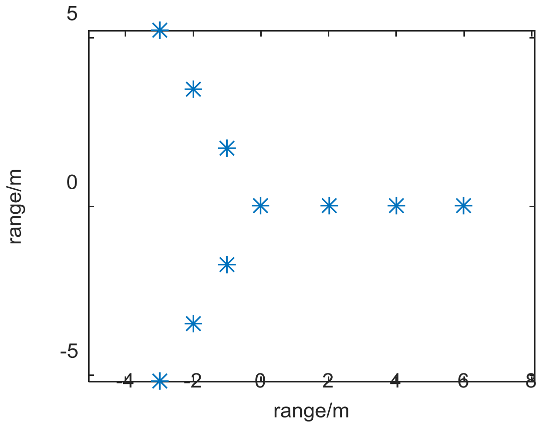

Figure 2. Model of rotor target

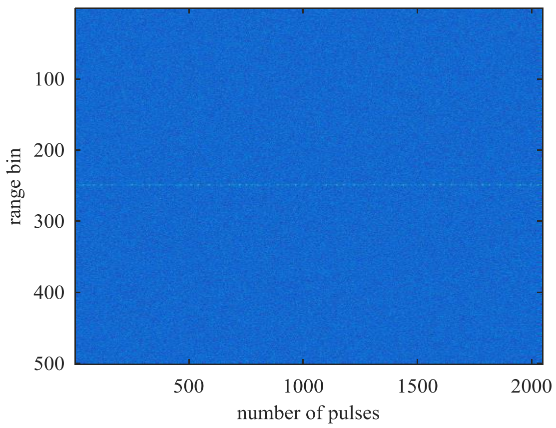

Figure 3. Simulated echo

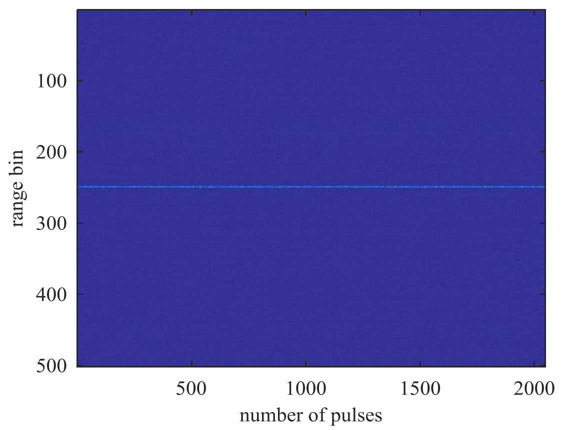

Figure 4. Range dimension denoising result

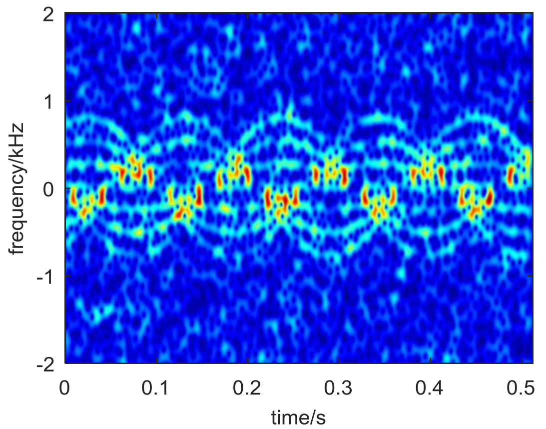

Figure 5. Time-frequency result before azimuth denoising

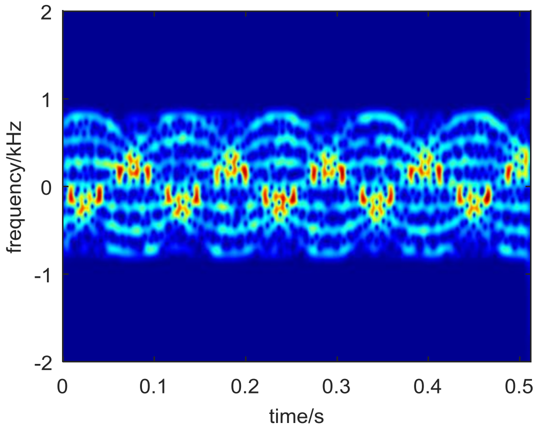

Figure 6. SSA denoising result

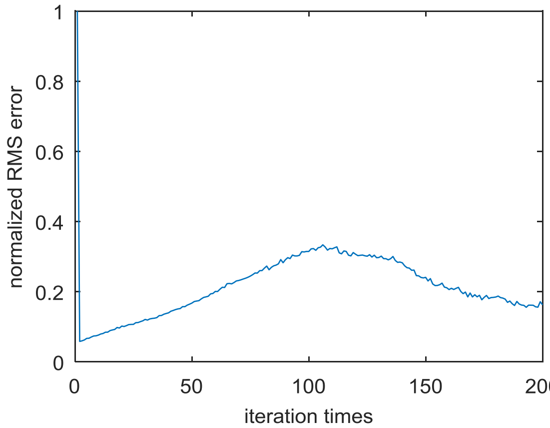

Figure 7. L2-RISK function

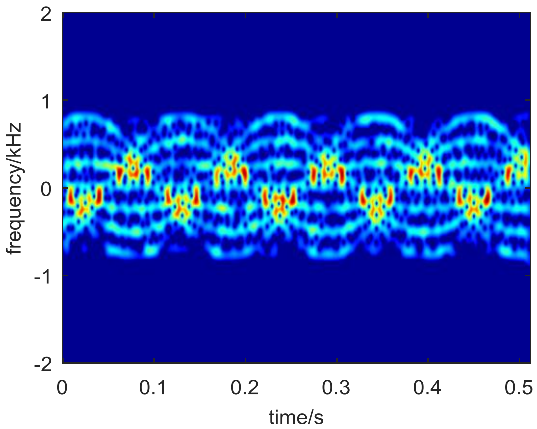

Figure 8. Time-frequency filtering denoise result

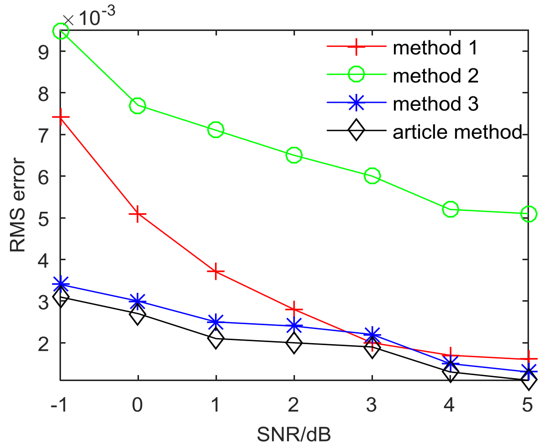

Figure 9. Performance comparison

As can be seen from Figure.3 and Figure.4, it is difficult to detect the range bin of the target at SNR=3dB, but after denoise algorithm in range dimension, the echo can be well denoised, and the rang bin of the target can be clearly obtained after denoising, but the SNR in this range bin will not change. From Figure.5, there is a lot of noise in the time-frequency results, so it is necessary to denoise in the azimuth dimension. From Figure.6, after SSA processing, the high-frequency noise which does not overlap with the frequencies of target signal can be removed completely, however, the noise with the same frequency as the target signal still remains. This is because the signal is reconstructed by choosing a larger singular value which is not completely contributed by the target signal, and there is still a small amount of noise. The denoise result is filtered by adaptive threshold time-frequency filtering, when the first local minimum value of the risk function curve in Figure.7 is taken, the denoise effect is the best. In Figure.8, not only the residual noise after SSA is eliminated to the greatest extent, but also the time-frequency characteristics of target are guaranteed to the greatest extent. From Fig.9, we can see that algorithm mentioned in this paper has better denoise performance than the traditional denoise algorithm.

5. Conclusion

(1) Through the analysis of noisy signal, it is shown that the weight function constructed by coherent accumulation and the weighted processing of the echo range dimension can effectively reduce the noise of the echo range dimension and detect the range bin of the target.

(2) Because of the non-stationary characteristic of the noisy fretting target signal, the effect of the traditional denoise algorithm is poor. Through simulation, the feasibility of the method based on SSA

and adaptive threshold time-frequency filtering is qualitatively illustrated. Compared with the traditional method, the time-frequency spectrum after denoise algorithm mentioned in this paper has better denoise performance.

References

[1] Alvanitopoulos P F, Papavasileiou M, Andreadis I, et al. Seismic Intensity Feature Construction Based on the Hilbert–Huang Transform[J]. IEEE Transactions on Instrumentation & Measurement, 2012, 61(2):326-337.
[2] Beenamol M, Prabavathy S, Mohanalin J. Wavelet based seismic signal de-noising using Shannon and Tsallis entropy[J]. Computers & Mathematics with Applications, 2012, 64(11):3580-3593.
[3] Gaci S. The Use of Wavelet-Based Denoising Techniques to Enhance the First-Arrival Picking on Seismic Traces[J]. IEEE Transactions on Geoscience & Remote Sensing, 2014, 52(8):4558-4563.
[4] Chatlani N, Soraghan J J. EMD-Based Filtering (EMDF) of Low-Frequency Noise for Speech Enhancement[J]. IEEE Transactions on Audio Speech & Language Processing, 2012, 20(4):1158-1166.
[5] Yue L I, Peng J L, Hai-Tao M A. Study of the influence of transition IMF on EMD do-noising and the improved algorithm[J]. Acta Geophysica Sinica, 2013, 56(2):626-634.
[6] Rato R T, M.D. Ortigueira, Batista A G. On the HHT, its problems, and some solutions[J]. Mechanical Systems & Signal Processing, 2008, 22(6):1374-1394.
[7] Jia R S, Zhao T B, Sun H M, et al. Micro-seismic signal denoising method based on empirical mode decomposition and independent component analysis[J]. Chinese Journal of Geophysics, 2015, 58(3):1013-1023.
[8] Chen R X, Tang B P, Ma J H. Adaptive de-noising method based on ensemble empirical mode decomposition for vibration signal[J]. Journal of Vibration & Shock, 2012, 31(15):82-86.
[9] Chen R, Tang B, Lu Zhongliang. Ensemble Empirical Mode Decomposition De-noising Method Based on Correlation Coefficients for Vibration Signal of Rotor System[J]. Journal of Vibration Measurement & Diagnosis, 2012, 32(4):542-546.
[10] Xia X G. System identification using chirp signals and time-variant filters in the joint time-frequency domain[J]. IEEE Transactions on Signal Processing, 1997, 45(8):2072-2084.
[11] Guo Y, Wei Y, Zhou X. Signal denoising method based on STFT time-frequency spectrum coefficients shrinkage[J]. Journal of Vibration Measurement & Diagnosis, 2015(6):1090-1096.
[12] Chen Yong-Bin, Li Shao-Dong, Yang Jun, Cao Fu-Rong. Rotor blades radar echo modeling and its mechanism analysis[J]. Acta Physica Sinica, 2016, 65(13): 138401.
[13] Chen Y, Shaodong L I, Yang J, et al. A New Method for Micro-Motion Signature Extraction of Rotor Blades[J]. Radar Science & Technology, 2017,15(1): 13-18.
[14] Ya-An L I, Wang H C, Jing C. Research of noise reduction of underwater acoustic signals based on singular spectrum analysis[J]. Systems Engineering & Electronics, 2007, 29(4):524-527.
[15] Sun X. Noise Reduction of Frequency Response Function Using Singular Value Decomposition[J]. Journal of Vibration Measurement & Diagnosis, 2009, 29(3):325-328.
[16] Qian Z, Li C, Li Y. Noise Reduction Method Based on Singular Value Decomposition[J]. Journal of Vibration Measurement & Diagnosis, 2011, 31(4):459-463.
[17] Song J, Yu L, Wang X D. Improved denoising algorithm for narrow-band signal and its application[J]. Journal of Vibration & Shock, 2013, 32(16): 59-63.